Orbitronics: The Intrinsic Orbital Current in p-Doped Silicon

B. Andrei Bernevig, Taylor L. Hughes, and Shou-Cheng Zhang
Department of Physics, Stanford University, Stanford, California 94305, USA
(Received 14 February 2005; published 1 August 2005)

The spin Hall effect depends crucially on the intrinsic spin-orbit coupling of the energy band. Because of the smaller spin-orbit coupling in silicon, the spin Hall effect is expected to be much reduced. We show that an electric field in p-doped silicon can induce a dissipationless orbital current in a fashion reminiscent of the spin Hall effect. The vertex correction from impurity scattering vanishes and the effect is robust against disorder. The orbital Hall effect leads to accumulation of local orbital momentum at the edge of the sample, and can be detected by the Kerr effect.

DOI: 10.1103/PhysRevLett.95.066601 PACS numbers: 72.25.Dc, 72.25.Hg, 73.43.−f, 85.75.−d

Spin manipulation in semiconductors has seen remarkable theoretical and experimental interest in recent years with the advent of spin electronics, and with the realization that strong spin-orbit coupling in certain materials can influence the transport of carriers in spintronics devices [1]. A new way to manipulate spin has recently been proposed, where the spin current is created by an electric field through the intrinsic spin-orbit coupling in the semiconductor bands [2,3]. The direction of the spin polarization, the current flow, and the electric field are mutually perpendicular. The spin Hall effect has been recently observed experimentally [4,5].

Possibly of great application in semiconductors with large spin-orbit coupling such as GaAs and InSb, the effect is expected to be smaller in the most used semiconductor of the electronics industry: silicon. The small spin-orbit coupling in silicon, as measured by the energy of the split-off band relative to the top of the valence band, ~44 MeV, makes the spin Hall effect small at room temperature. Recently, Yao *et al.* [6] computed the spin Hall effect for a variety of materials, and found that the spin Hall effect of Si is smaller than GaAs.

Given the dominance of silicon in the semiconductor industry, it is important to find a similar dissipationless transport process which does not rely on the spin-orbit coupling. In this Letter, we investigate the possibility of replacing the spin degree of freedom by the orbital degree of freedom, and call the associated field of study orbitronics. Although the effects of orbital charge currents in response to an electric field have been studied [7,8], an orbital angular-momentum current is novel in the spintronics field. The valence band of Si (Fig. 1) consists of three p orbitals. The three orbital degrees of freedom transform as a (pseudo-) spin one quantity under rotation, are odd under time reversal, and couple to the crystal momentum of the hole. We show that p-doped Si under the influence of an electric field develops an intrinsic orbital current of the p band. The polarization of the p orbitals, the direction of flow, and the direction of the electric field are mutually perpendicular:

$$j^i_j = \sigma_I \epsilon_{ijk} E_k. \tag{1}$$

Here j^i_j stands for the orbital current flowing along the j direction, where the local orbitals are polarized along the i direction. For an electric field on the y axis, we expect an orbital current flowing in the positive(negative) x direction to be polarized in the $+z = p_x + ip_y (-z = p_x - ip_y)$ direction. Like the spin current, the orbital current is also even under time reversal, and the above response equation is dissipationless.

As a semiconductor with diamond structure the valence band of Si contains 3 p orbitals where the holes reside [9]. While in most semiconductors the intrinsic spin-1/2 of the holes couples with the spin-1 p orbitals to create the light and heavy hole bands as well as the split-off band, in silicon this coupling is small and its energy scale is easily overtaken by disorder or thermal fluctuations. We therefore neglect it. The diamond lattice symmetry therefore requires that the form of the Hamiltonian near the zone center be [10,11]

$$H = Ak^2 - (A - B)\sum_{i=1}^{3} k_i^2 I_i^2 - \frac{C}{2}\sum_{i\neq j=1}^{3} \{k_i, k_j\}\{I_i, I_j\} \tag{2}$$

where the I_i are the orbital angular momentum matrices:

$$I_x = \begin{pmatrix} 0 & 1 & 0 \\ 1 & 0 & 1 \\ 0 & 1 & 0 \end{pmatrix} \quad I_y = \begin{pmatrix} 0 & -i & 0 \\ i & 0 & -i \\ 0 & i & 0 \end{pmatrix} \quad I_z = \begin{pmatrix} 1 & 0 & 0 \\ 0 & 0 & 0 \\ 0 & 0 & -1 \end{pmatrix},$$

and A, B, C are material constants. An essential feature of the above Hamiltonian is the coupling between the local orbital moment I_i and the momentum k_i. In analogy with the spin-orbit coupling we call this orbital-orbit coupling. In the spherical approximation ($A - B = C$)

$$H = Ak^2 - r(\vec{k}\cdot\vec{I})^2, \tag{3}$$

where we have defined $r \equiv A - B$ to simplify notation. This form is identical to the spherically symmetric Luttinger Hamiltonian for the light and heavy hole bands, but as a fundamental physical (and mathematical) difference, the matrix I is not a spin-3/2 4×4 matrix but spin-1 p orbital 3×3 matrices. For simplicity, we now work with the spherically symmetric Hamiltonian.

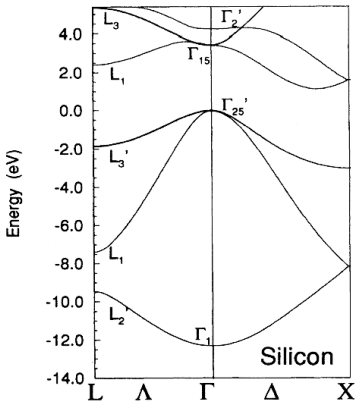

FIG. 1. Si energy bands [23]. The effective Hamiltonian in Eq. (3) describes the Γ'_{25} bands close to the Γ point.

Good quantum numbers are helicity $\lambda = \vec{k}\cdot\vec{I}/k$ and total angular momentum $\vec{J} = \vec{x}\times\vec{p} + \vec{I}$, which is a sum of motion angular momentum plus localized orbital momentum. There are two degenerate bands of helicity $\lambda = \pm 1$ and a third of helicity $\lambda = 0$; $\epsilon_{\pm 1}(k) = Ak^2$, $\epsilon_0(k) = (A - r)k^2$. Introducing five matrices [12] ξ^{ij}_a, where $a = 1\ldots 5$, $i, j = 1, 2, 3$, $\xi^{ij}_a = \xi^{ji}_a$ and $\xi^{ii}_a = 0$, Eq. (3) is

$$H(k) = \epsilon(k) + r(d_a\Gamma^a), \tag{4}$$

$$\epsilon(k) = \frac{k^2}{3}(3A - 2r), \quad d_a(k) = \xi^{ij}_a k_i k_j, \quad \Gamma_a = \xi^{ij}_a I_i I_j,$$
$$d_1 = -\sqrt{3}k_y k_z, \quad d_2 = -\sqrt{3}k_x k_z, \quad d_3 = -\sqrt{3}k_x k_y \tag{5}$$
$$d_4 = -\frac{\sqrt{3}}{2}(k_x^2 - k_y^2), \quad d_5 = -\frac{1}{2}(2k_z^2 - k_x^2 - k_y^2).$$

Following Ref. [12], one can similarly define the so-called conserved spin, i.e., the orbital operator projected onto the eigenstate bands of the model. Using the projection operators onto the helicity bands in terms of the Γ^a: $P_{\lambda^2=1} = (\hat{k}\cdot I)^2 = \frac{2}{3} - \frac{1}{k^2}d_a\Gamma^a$, $P_{\lambda^2=0} = 1 - P_{\lambda^2=1}$ (with the projection operator properties $P_0^2 = P_0$, $P_{\pm 1}^2 = P_{\pm 1}$, $P_0 P_{\pm 1} = 0$), the Hamiltonian can be written as $H = \epsilon_{\pm 1}(k)P_{\pm 1}(k) + \epsilon_0(k)P_0(k)$. The conserved local orbital moment operator, $I_i^{\rm con} = P_0 I_i P_0 + P_1 I_i P_1$ then commutes with H. The conserved orbital moment formalism physically implies that we consider the system in its adiabatic state, where changes to the equilibrium state, such as applied fields, etc., are slow enough as to maintain the system in its energy eigenstates. It is also the case that the local orbital moment operator I_i has no projection onto the zero-helicity band, i.e., $P_0 I_i P_0 = 0$. The projected motion of local orbital moments is equivalent to the projection onto the degenerate helicity $\lambda = \pm 1$ bands.

We now consider the effect of a uniform electric field $\vec{E}$, with potential $V(x) = e\vec{E}\cdot\vec{x}$. The field accelerates the particles but, since the momentum k_i is coupled to the local orbital moment I^i, the electric field will influence its motion and orientation. In particular, a nonzero local orbital current appears which selectively polarizes moving electrons into certain p orbitals.

One can define two orbital currents, though one is perhaps more appropriate. First we have the conventional orbital-current given by $J^i_j = \frac{1}{2}\{\frac{\partial H}{\partial k_j}, I^i\}$ with the brackets denoting an anticommutator. This current is not conserved by the Hamiltonian dynamics and thus a more appropriate current to consider is that given by the motion of the conserved orbital moment $J^i_{j(c)} = \frac{1}{2}\{\frac{\partial H}{\partial k_j}, P_0 I^i P_0 + P_1 I^i P_1\} = \frac{1}{2}\{\frac{\partial H}{\partial k_j}, P_1 I^i P_1\}$. This conserved current is the current of the orbital moment in the helicity ± 1 band.

The Green's function for the above Hamiltonian is matrix-valued: $G(E, k) = (E - (\epsilon(k) + (A - B)d_a\Gamma^a))^{-1}$. The lack of a Clifford-algebra property for the 3×3 Γ^a matrices makes the solution of this inversion hard. After tedious algebra we find

$$G(E, k) = \frac{3(rk^2 - 3E(k)) - 9rd_a\Gamma^a}{(-3E(k) + 2rk^2)(3E(k) + rk^2)}, \tag{6}$$

with $E(k) \equiv E - \epsilon(k)$. We compute the response of the orbital current to an electric field, from the Kubo formula: $Q^l_{ij}(i\nu_m) = \frac{1}{V\beta}\Sigma_{k,n}\,\mathrm{Tr}[J^l_i G(i(\omega_n + \nu_m), k) J_j G(i\omega_n, k)]$ with Matsubara frequencies $\nu_m = 2\pi m/\beta$, $\omega_n = (2n+1)\pi/\beta$, and charge current operator $J_j = \partial H/\partial k^j$. After performing the summation over the Matsubara frequencies, we find, for example, the Q^1_{23} component for the conserved current is given by

$$Q^1_{23}(i\nu_m) = -\frac{1}{V}\sum_k \frac{(n_F(\epsilon_{\pm 1}) - n_F(\epsilon_0))r^2 k_x^2 \nu_m}{2((i\nu_m)^2 - r^2k^4)}, \tag{7}$$

where n_F is the Fermi-Dirac distribution function. The next step is to consider the zero-frequency limit of the orbital conductivity which is obtained from the response function as $\sigma^l_{ij} = \lim_{i\nu_m\to 0}\frac{Q^l_{ij}(i\nu_m)}{\nu_m}$. After the momentum integration, we obtain a beautiful tensor structure:

$$\sigma^i_{jk} = \epsilon_{ijk}\sigma_I. \tag{8}$$

It is especially suggestive that this tensor structure is identical to the one in the spin Hall effect [2] although the gauge (matrix) structure of the Hamiltonian is fundamentally different. The conductivity σ_I is

$$\sigma_I = 2\int_{k_0^F}^{k_{\pm 1}^F}\frac{d^3k}{(2\pi)^3}\frac{k_x^2}{k^4} = \frac{1}{3\pi^2}(k^F_{\pm 1} - k^F_0). \tag{9}$$

$k^F_{\pm 1,0}$ are the Fermi momenta of the two bands. An identical picture emerges if we consider the response of the nonconserved orbital current to an electric field, the only difference being in the value of the constant σ_I which in the nonconserved case is $\sigma_I = \frac{1}{6\pi^2}(\frac{5}{3} + 4\frac{A}{A-B})(k^F_{\pm 1} - k^F_0)$. Estimates for orbital and charge conductivities of Si at a given carrier density are given in Table I. These calculations assume the mobility of holes in Si is 450 $\mathrm{cm}^2/\mathrm{V\,s}$ [13]. In this computation we have made 3 approximations. The first approximation is the neglect of the Si spin-orbit (SO) coupling. As commented at the beginning of the

TABLE I. Values are a function of the density n. We have orbital conductivity σ_I, charge conductivity σ_c, spin diffusion length l, energy difference between the two hole bands at Fermi energy ΔE, and orbital polarization density ρ_I.

$n(\mathrm{cm}^{-3})$	$\sigma_I(\frac{1}{\Omega\cdot\mathrm{cm}})$	$\sigma_c(\frac{1}{\Omega\cdot\mathrm{cm}})$	$l(\mu\mathrm{m})$	$\Delta E(\mathrm{meV})$	$\rho_I(\frac{\mu_B}{\mathrm{cm}^2})$
10^{21}	82.8	72 000	3.9	540	2×10^{15}
10^{20}	38.6	7200	1.8	120	9×10^{14}
10^{19}	17.9	720	0.85	24	4×10^{14}
10^{18}	8.28	72	0.39	5.4	2×10^{14}
10^{17}	3.86	7.2	0.18	1.2	9×10^{13}
10^{16}	1.77	0.72	0.085	0.25	4×10^{13}

Letter, the Si SO coupling is small (44 MeV) and is likely to be suppressed by the energy scales of disorder and temperature. The energy scale at room temperature is of the same order of magnitude as the Si SO coupling ~26 MeV, while the difference of energies between $\epsilon_{\pm1}$, ϵ_0 bands at the Fermi energy is much larger, e.g., $\Delta E \sim 120$ MeV at $n = 10^{20}/\mathrm{cm}^3$ (refer to Table I for values at other densities). Hence the orbital effect proposed here is much larger than any spin Hall effect that Si might have due to its small SO coupling. To substantiate our claims we perform a numerical computation of the temperature dependence of both the orbital Hall effect above and the spin Hall effect that Si would have had we not neglected the spin-orbit coupling. This is done by introducing temperature-dependent Fermi functions. The numerical results are presented in Fig. 2 for the orbital and spin Hall conductivities at two different doping levels. Both conductivities are more or less constant over a temperature range up to the difference in Fermi energies of the bands. Above that temperature, they fall down and vanish in the high-temperature limit where the bands are not well-defined. We can see that the orbital Hall effect (yellow and red curves) is much more robust and larger than its spin Hall counterpart.

Another caveat in this calculation is our neglect of anisotropy by using the spherical Hamiltonian to model Si. We assumed that $(A - B) \approx C$ for silicon though this is not true. When $((A - B) - C)/A$ is large we cannot form the rotationally invariant $(\vec{k}\cdot\vec{I})^2$ term and the problem is more challenging, allowing only a numerical solution. In Fig. 2 we plot the orbital Hall conductance as a function of the anisotropy parameter $(A - B)/C$. We see that for real Si parameters (see Table II) the orbital Hall conductance is

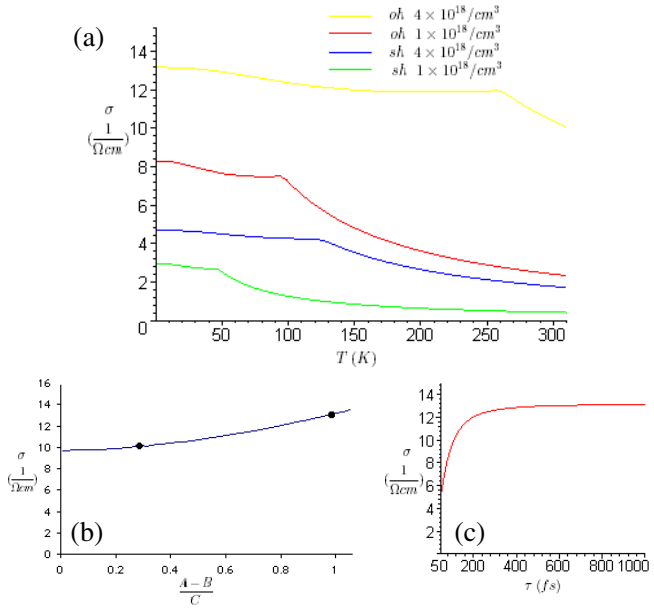

FIG. 2 (color online). (a) Temperature dependence of orbital Hall (oh) and spin Hall (sh) conductivities for values of the density. The (oh) effect is more robust than the (sh) effect. (b) Orbital Hall conductivity for anisotropic band structure at $n = 4\times10^{18}/\mathrm{cm}^3$. Dots represent the isotropic (real) parameters for Si, $(A - B)/C = 1(0.27)$. (c) Dependence of orbital Hall conductivity on disorder broadening for $n = 4\times10^{18}/\mathrm{cm}^3$. Down to $\tau \approx 100$ fs it is very robust.

$$\sigma_I(\xi) = \frac{-1}{24\pi^2}\left(-8k + \sqrt{2}\xi\ln\left[\frac{k^2+\sqrt{2}k\xi+\xi^2}{-k^2+\sqrt{2}k\xi-\xi^2}\right] + 2\sqrt{2}\left\{\arctan\left[\frac{\sqrt{2}k}{\xi}+1\right] + \arctan\left[\frac{\sqrt{2}k}{\xi}-1\right]\right\}\right)\Bigg|_{k_0}^{k_1} \tag{10}$$

where $\xi \equiv \sqrt{\hbar}/\sqrt{r\tau}$. Despite the unappealing form of this formula, its dependence on τ is expected. The orbital Hall conductance will remain approximately constant up to the point where τ becomes short enough to be comparable with the Fermi energy difference between the two bands. Afterwards, disorder will kill the orbital Hall effect. As smaller than in the spherical approximation, the error is about 20%.

The effect of impurities enters in two forms, as a vertex correction of the current operator and as a self-energy correction. In the context of the spin Hall effect, analytical calculations have shown that the spin Hall effect in the Rashba model [3] is cancelled by the vertex corrections due to impurity scattering [14–16]. However, the vertex correction vanishes identically [17] for the spin Hall effect in the Luttinger model describing the holes [2]. This is because the current vertex is odd under parity, while the Hamiltonian is even under parity. A similar argument is valid here: the orbital-current operator is odd under parity while the Hamiltonian is even. Thus, the vertex correction due to impurity scattering vanishes for the orbital Hall effect and should be robust. The self-energy correction is finite and can be computed by assuming a finite momentum relaxation time τ in the expression for the orbital Hall conductance ($\nu_m \to \hbar/\tau$).

plotted in Fig. 2 for $n = 4\times10^{18}$ cm^{-3}, this happens for $\tau < 100$ fs, not a worrisome number. The Fermi energy difference for this density is $\tau \sim 50$ fs.

For an electric field parallel to the y axis the transport equation is $J^i_j = \epsilon_{ijy}E_y$, and we have an orbital current flowing along $j = x$ with orbital local moment polarized in

TABLE II. Parameters for silicon [9,24], units are J m^2.

A	B	C	$A-B$
0.243×10^{-37}	0.386×10^{-37}	-0.527×10^{-37}	-0.143×10^{-37}

the $i=z$ direction. Since there is no net charge current in the xz plane, at a microscopic level there are an equal number of holes flowing in the $\pm x$ direction. However, the holes flowing in the $+x(-x)$ direction tend to populate more the $p_x+ip_y(p_x-ip_y)$ local orbitals so as to give a net $+z(-z)$ polarization. At one of the boundaries of the sample there will be a net accumulation of p_x+ip_y occupied orbitals while at the opposite end the holes will tend to occupy p_x-ip_y orbitals.

There have been several recent experiments that can detect spin currents via spin accumulation at the boundary [4,5] and these provide a basis for detecting the intrinsic orbital current in silicon. Since Si is an indirect-gap material with low efficiency for light emission, an LED-type experiment like [5], where the polarization of the emitted light would give information about the occupied orbital, is not viable. However, Kerr and Faraday rotation measurements are insensitive to the Si indirect gap and can be used to probe orbital polarization. As seen from the detection of the spin Hall effect in GaAs, the Kerr microscope is an effective experimental apparatus for spintronics. A similar experiment to [4] could be performed with Si. The orbital current will create two regions at the edge of the sample where electrons occupy orbitals polarized in opposite directions and will have different optical properties with respect to circularly polarized light. The change in the angle of the beam reflected from the surface of the sample gives information about the orbital moment polarized on the direction of the beam. The resolution of the Kerr microscope in [4] is $\approx 1\ \mu$m and must be comparable to the size of the region where the orbitally polarized electrons accumulate. This size is $L=\sqrt{D\tau_0}$ where τ_0 is the orbital-relaxation time. D is the hole diffusion coefficient $v_F^2\tau/3$ where τ is the momentum relaxation time, and v_F is the Fermi velocity. We know of no systematic studies of the orbital relaxation in Si, so we take the hole-spin relaxation time as a rough estimate, since these two quantities transform the same way, and couple to the crystal momentum in the same way. The size of the orbital polarization region depends heavily on the hole-spin relaxation times which are measured in semiconductors to be anywhere from $\tau_s\approx 4$ ps [18] to $\tau_s\approx 1$ ns [19]. Hole-spin relaxation times for Si structures have been measured to be on the order of $\sim$10 ps at low temperatures [20,21]. However, these measurements are ''bipolar'' measurements where both electrons and holes are excited and spin-polarized. A ''monopolar'' spin measurement, which excites carriers in intraband/intrasubband transitions, measures spin relaxation times without electron-hole interaction and exciton formation [22]. In this regime of intraband/intersubband transitions for p-type quantum wells a hole-spin lifetime of $\sim$30 ps is measured [22]. This value is the most relevant for our calculations so we use it in our estimations. We estimate the hole-spin diffusion constant (which we expect to be close to the orbital diffusion constant) and the spatial distribution of the orbital moments. The values for the hole-distribution length are given in Table I as l. For a steady electric current J_y we estimate the orbital-current density to be $j_I\sim(\sigma_I/\sigma_c)J_y$ [2]. The values of orbital polarization density are given by $j_I\tau_s$ [2]. Assuming 3×10^5 V/cm is an upper bound for the electric field in Si [13], we list values of the maximum orbital polarization density in Table I as ρ_I.

We thank Professor Z. Fang for numerous discussions on the subject. B. A. B. acknowledges support from the SGF Program. T. L. H. acknowledges support from the NSF Graduate Program. This work is supported by the NSF under Grant Nos. DMR-0342832 and the U.S. Department of Energy, Office of Basic Energy Sciences under Contract No. DE-AC03-76SF00515.

[1] S. A. Wolf *et al.*, Science **294**, 1488 (2001).
[2] S. Murakami, N. Nagaosa, and S. Zhang, Science **301**, 1348 (2003).
[3] J. Sinova *et al.*, Phys. Rev. Lett. **92**, 126603 (2004).
[4] Y. K. Kato *et al.*, Science **306**, 1910 (2004).
[5] J. Wunderlich *et al.*, cond-mat/0410295.
[6] Y. G. Yao *et al.*, Phys. Rev. Lett. **94**, 047204 (2005).
[7] J. Mertsching, Phys. Status Solidi **14**, 3 (1966).
[8] J. Mertsching, Phys. Status Solidi **26**, 9 (1968).
[9] J. M. Luttinger, Phys. Rev. **102**, 1030 (1956).
[10] J. M. Luttinger and W. Kohn, Phys. Rev. **97**, 869 (1955).
[11] H. Ehrenreich and A. W. Overhauser, Phys. Rev. **104**, 331 (1956).
[12] S. Murakami, N. Nagaosa, and S. C. Zhang, Phys. Rev. B **69**, 235206 (2004).
[13] *Handbook Series on Semiconductor Parameters*, edited by M. Levinstein, S. Rumyantsev, and M. Shur (World Scientific, Singapore, 1996).
[14] R. Raimondi *et al.*, Phys. Rev. B **64**, 235110 (2001).
[15] P. Schwab and R. Raimondi, Eur. Phys. J. B **25**, 483 (2002).
[16] J. I. Inoue, G. Bauer, and L. Molenkamp, Phys. Rev. B **70**, 041303(R) (2004).
[17] S. Murakami, Phys. Rev. B **69**, 241202(R) (2004).
[18] T. C. Damen *et al.*, Phys. Rev. Lett. **67**, 3432 (1991).
[19] Ph. Roussignol *et al.*, Surf. Sci. **267**, 360 (1992).
[20] G. M. Gusev, Z. D. Kvon, and V. N. Ovsyuk, J. Phys. C **17**, L683 (1984).
[21] V. V. Andrievskii *et al.*, Low Temp. Phys. **29**, 318 (2003).
[22] S. D. Ganichev *et al.*, Phys. Rev. Lett. **88**, 057401 (2002).
[23] G. Grosso and C. Piermarocchi, Phys. Rev. B **51**, 16 772 (1995).
[24] P. Lawaetz, Phys. Rev. B **4**, 3460 (1971).